



ELSEVIER

Contents lists available at ScienceDirect

## Deep-Sea Research II

journal homepage: [www.elsevier.com/locate/dsr2](http://www.elsevier.com/locate/dsr2)

## Seasonal evolution of the upper-ocean adjacent to the South Orkney Islands, Southern Ocean: Results from a “lazy biological mooring”

Michael P. Meredith<sup>a,\*</sup>, Keith W. Nicholls<sup>a</sup>, Ian A. Renfrew<sup>b</sup>, Lars Boehme<sup>c</sup>,  
Martin Biuw<sup>c,1</sup>, Mike Fedak<sup>c</sup>

<sup>a</sup> British Antarctic Survey, High Cross, Madingley Road, Cambridge CB3 0ET, UK

<sup>b</sup> School of Environmental Sciences, University of East Anglia, Norwich NR4 7TJ, UK

<sup>c</sup> Sea Mammal Research Unit, Scottish Oceans Institute, University of St Andrews, St Andrews KY16 8LB, UK

## ARTICLE INFO

## Article history:

Received 22 October 2008

Received in revised form

19 June 2009

Accepted 14 July 2009

## Keywords:

South Orkney Islands

Southern Ocean

Weddell–Scotia Confluence

Upper-ocean seasonality

Sea ice production

Air–sea–ice interaction

Elephant seal

## ABSTRACT

A serendipitous >8-month time series of hydrographic properties was obtained from the vicinity of the South Orkney Islands, Southern Ocean, by tagging a southern elephant seal (*Mirounga leonina*) on Signy Island with a Conductivity–Temperature–Depth/Satellite-Relay Data Logger (CTD–SRDL) in March 2007. Such a time series (including data from the austral autumn and winter) would have been extremely difficult to obtain via other means, and it illustrates with unprecedented temporal resolution the seasonal progression of upper-ocean water mass properties and stratification at this location. Sea ice production values of around 0.15–0.4 m month<sup>-1</sup> for April to July were inferred from the progression of salinity, with significant levels still in September (around 0.2 m month<sup>-1</sup>). However, these values presume that advective processes have negligible effect on the salinity changes observed locally; this presumption is seen to be inappropriate in this case, and it is argued that the ice production rates inferred are better considered as “smeared averages” for the region of the northwestern Weddell Sea upstream from the South Orkneys. The impact of such advective effects is illustrated by contrasting the observed hydrographic series with the output of a one-dimensional model of the upper-ocean forced with local fluxes. It is found that the difference in magnitude between local (modelled) and regional (inferred) ice production is significant, with estimates differing by around a factor of two. A halo of markedly low sea ice concentration around the South Orkneys during the austral winter offers at least a partial explanation for this, since it enabled stronger atmosphere/ocean fluxes to persist and hence stronger ice production to prevail locally compared with the upstream region. The year of data collection was an El Niño year, and it is well-established that this phenomenon can impact strongly on the surface ocean and ice field in this sector of the Southern Ocean, thus the possibility of our time series being atypical cannot be ruled out. Longer-term collection of *in situ* ocean data from this locality would be desirable, to address issues relating to interannual variability and long-term change.

© 2011 Elsevier Ltd. All rights reserved.

### 1. Introduction

The South Orkney Islands reside on the South Scotia Ridge, separating the Weddell Sea to the south from the Scotia Sea to the north (Fig. 1). Oceanographically this is a complex region, lying between the waters of the Antarctic Circumpolar Current (ACC) and those of the Weddell Gyre. The ACC is delineated to the south by the Southern Boundary (SB; Fig. 1), whilst the northern edge of the Weddell Gyre is marked by the Weddell Front (WF). In between these two features lie the waters of the Weddell–Scotia Confluence (WSC), which are characterised by lower vertical gradients in properties compared with waters either side,

a consequence of the injection of dense waters that spill from the tip of the Antarctic Peninsula and flow eastward at mid-depths (Whitworth et al., 1994). The waters of the WSC are also notable for having high concentrations of chlorophyll in response to seasonal phytoplankton blooms (Korb et al., 2004), despite the general High Nutrient Low Chlorophyll (HNLC) characteristics of the broader Southern Ocean in general (Falkowski et al., 1998). This is presumed to be due to the advective supply of micronutrients (especially iron) from the Antarctic Peninsula and their upward mixing from the South Scotia Ridge seamounts, highlighting the key role of physical processes in determining biogeochemical distributions in this region (e.g. Korb et al., 2005).

In common with many areas of the Southern Ocean, our understanding of physical processes near the South Orkney Islands has been hampered by a general paucity of *in situ* observations. Much of the understanding that has been generated has been the result of research cruises conducted in the austral

\* Corresponding author.

E-mail address: [mmm@bas.ac.uk](mailto:mmm@bas.ac.uk) (M.P. Meredith).

<sup>1</sup> Now at: Polar Environmental Centre, Norwegian Polar Institute, NO-9296 Tromsø, Norway.

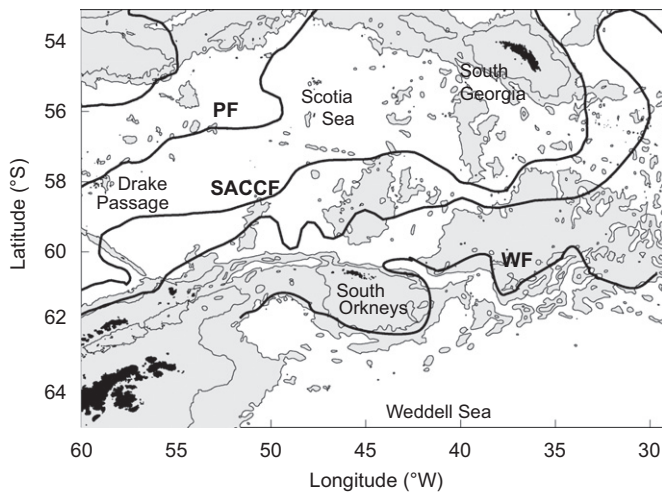


**Fig. 1.** Location of the South Orkney Islands on the South Scotia Ridge, between the Weddell Sea and Scotia Sea. The 1000 and 3000 m isobaths are marked; regions shallower than 3000 m are shaded. Fronts of the ACC are marked (Polar Front, PF; Southern ACC Front, SACCF), as is the southernmost limit of the ACC (Southern Boundary, SB). The Weddell Front (WF), marking the southern limit of the Weddell–Scotia Confluence is shown. Frontal locations are taken from Orsi et al. (1995) and Heywood et al. (2004).

summer, and these have been used to document water mass distributions, quantify mixing and track advective flow paths (e.g. Muench and Hellmer, 2002; Muench et al., 2002; Heywood et al., 2004). In contrast, the austral winter has been very significantly undersampled in this region, and this has restricted progress in understanding the seasonal evolution of the upper ocean water masses, and their interactions with the sea ice field.

A significant exception to this is the monitoring work conducted from Signy Island, in the South Orkneys, between 1988 and 1994 (Clarke and Leakey, 1996, building on previous work by Clarke, 1988). These workers made weekly measurements of temperature, chlorophyll and other biological parameters from a coastal site (water depth around 25 m), and documented significant seasonal and interannual variability in the data obtained. The water column was observed to be generally well-mixed at the shallow site of sampling, hence data were collected from a single depth instead of vertical profiles being collected. Peak seawater temperatures varied between 0 and 2 °C in summer, and a significant relationship between summer temperatures and winter fast-ice duration was observed, whereby long periods of fast-ice were followed by colder summer seawater temperatures.

The fast-ice records from Signy Island date back to 1947, allowing a long-term perspective on variability and change in this region. The winter fast-ice duration was observed to vary between 0 days (in 1956) and 219 days (in 1949 and 1966), with a median value of 119 days (Murphy et al., 1995; Clarke and Leakey, 1996). In terms of interannual variability, a distinct cyclicity (of period 7–9 years) existed between the mid-1960s and late 1980s, but was absent outside of this period. This cyclicity has been linked to a large-scale precessional mode of climate variability that influenced the Southern Ocean circumpolarly for this period (Murphy et al., 1995), though the cause of the longer-period variability in the prevalence of this mode is not fully determined (e.g. Connolley, 2002).

The above studies have illustrated a coupling between the sea ice and ocean in this vicinity, and have demonstrated the need for greater year-round *in situ* data coverage with which to progress our understanding of these issues. However, this is one of the most challenging environments from which to collect year-round data. Previous collection of such data was made possible due to

the presence of a continuously manned research station on Signy Island, operated by the British Antarctic Survey. With the Signy station switching to be a summer-only operation in the 1990s, the collection of *in situ* wintertime measurements here has become problematic. In particular, repeat oceanographic measurements using Conductivity–Temperature–Depth (CTD) profilers are no longer possible in winter, since they require manual operation. Oceanographic moorings can obtain data year-round, even in ice-covered regions (e.g. Moffat et al., 2008), and can profile acoustically to the surface. However, if the moorings themselves extend to the near-surface layers (where coupling with sea ice occurs), which is necessary for temperature and salinity measurements, they become vulnerable to damage and destruction by the sea ice. Recent developments with profiling floats have led to a system that is capable of collecting hydrographic profiles in seasonally ice-covered seas (Klatt et al., 2007), and whilst these measurements are undoubtedly valuable, the Lagrangian nature of the floats' behaviour means that the locations of data return cannot be predetermined, nor can planned repeat measurements from a given location be undertaken.

In this paper, we present results from a novel and serendipitous monitoring exercise that provided the first quasi-Eulerian near year-round profiling of the upper ocean close to the South Orkney Islands. The measurements were obtained from miniaturised CTD instrumentation attached to a southern elephant seal (*Mirounga leonina*) that reported data in real-time via satellite. Technology of this genre has been available for some time, but recent developments and advances (Lydersen et al., 2002; Fedak, 2004; Lydersen et al., 2004) have enabled some significant new insights into both physical oceanography and the nature of marine mammal behaviour. In the Southern Ocean context, Biuw et al. (2007) examined the behaviour and condition of southern elephant seals and found distinct relationships with horizontal oceanographic zonation and vertical water mass layering, whilst Charrassin et al. (2008) used seal-derived data alongside other data sets to map the circumpolar fronts in the Southern Ocean with unprecedented resolution, and also to investigate sea ice production rates in certain areas. Costa et al. (2008) used a comprehensive dataset from seals tagged at the west Antarctic Peninsula to investigate physical variability and heat fluxes at this location, and Boehme et al. (2008a, 2008b) examined changes in the spatial structure and transport of the ACC using data from seals tagged on South Georgia. By implementing this technology at the South Orkneys, we recovered a unique (if unplanned) time series that includes profiles that extend to the surface during austral autumn and winter. We use these data to elucidate the seasonal evolution of the water column in this locale, and its interaction with the regional sea ice field.

## 2. Methods

### 2.1. *In situ* oceanographic data collection

Hydrographic data in this study were collected using a CTD Satellite-Relay Data Logger (CTD–SRDL), manufactured by the Sea Mammal Research Unit (SMRU) of the University of St. Andrews and Valeport Ltd. (UK). This was attached to a southern elephant seal after its moult on Signy Island in the South Orkneys in March 2007 (Fig. 2), and remained in place until November 2007, thereby yielding over 8 months of *in situ* data.

The sensor package included a Keller PA-7 pressure transducer (accuracy  $\pm 5$  dbar), a custom-made temperature probe (resolution  $\pm 0.001$  °C, accuracy 0.01 °C) and an inductive coil for measuring conductivity (resolution  $\pm 0.003$  mS cm<sup>-1</sup>). Profile data were collected during the animal's dives, and relayed via Argos



**Fig. 2.** The Southern elephant seal (*Mirounga leonina*) that was tagged on Signy Island in the South Orkneys with a SMRU CTD-SRDL in March 2007. Not the intrepid adventurer that we had hoped for.

satellite system. Because of constraints due to Argos bandwidth, not all the profile information could be transmitted. Instead, 18 data points were transmitted in two Argos messages, with 10 depths chosen from a table depending on maximum dive depth, and 8 chosen by a broken-stick method to best represent the shape of the profile based on its inflection points. Approximately 2.6 profiles per day were recovered using this technique, with the mean depth of profiling being around 400 m.

The CTD-SRDL instruments are increasingly being used on deep-diving and long-ranging animals to collect *in situ* hydrographic profile data from wide spatial areas that cannot be covered by research ships alone, and to collect data from regions that are not amenable to research ship operations (Boehme et al., 2008a, 2008b; Charrassin et al., 2008; Costa et al., 2008; Roquet et al., 2009). They complement the relatively recent Argo float programme, with the added feature of a biologically determined profiling and ranging pattern, which, as will be seen, can provide a usefully different profiling regime.

When the elephant seal was tagged on Signy Island, it was hoped that this animal would range deeply into the ice-covered Weddell Sea in winter, thereby providing data from a region inaccessible to ships and from which very few hydrographic measurements have been collected. Unfortunately, the specific elephant seal that was tagged (Fig. 2) was not quite the enthusiastic adventurer that we had hoped for, choosing instead to spend the following months very close to the South Orkneys, and venturing only briefly beyond the shelf slope adjacent to these islands. This behaviour seems to be a consequence of the particular elephant seal chosen being a benthic forager, as

opposed to an open-ocean frontal forager or an ice-related forager. Therefore, instead of the wide-ranging data coverage that we had hoped for, we obtained instead a near-perfect Eulerian time series adjacent to the South Orkneys. The data are interpreted here in this context.

## 2.2. Atmospheric and sea ice data

Atmospheric observations were obtained from Orcadas Station (WMO station 88968) on Laurie Island in the South Orkneys. These included mean sea-level pressure, 10 m wind speed and direction, 2 m air temperature, 2 m dewpoint temperature (providing a measure of humidity) and cloud fraction, each at 6 h intervals. Precipitation is problematic to measure directly in this region, due to the difficulty in distinguishing incident precipitation from wind-blown snow. Hence precipitation data used here were extracted from the European Centre for Medium-Range Weather Forecast's (ECMWF) operational analyses for a gridpoint just north of the South Orkney Islands. Sea surface temperature (SST) data were also extracted from ECMWF operational analyses.

To calculate a surface energy budget for Signy, the total heat flux from the ocean into the atmosphere,  $Q_{tot}$ , was derived as  $Q_{tot} = Q_s + Q_l + Q_r$ , where  $Q_s$  is the sensible heat flux,  $Q_l$  is the latent heat flux and  $Q_r$  is the net radiative heat flux. The turbulent heat fluxes were calculated using a stability-dependent algorithm based on Smith (1988) and DeCosmo et al. (1996). Long wave and short wave radiative fluxes were calculated from well-established empirical formulae using SST, air temperature, humidity and cloud cover as input data (see Renfrew et al. (2002) for details of surface flux calculations).

Sea ice concentration data used for ice production modelling purposes (see below) and for broader-scale contextualising of the oceanographic data were obtained from the Special Scanning Microwave Imager (SSM/I) on the Defense Meteorological Satellite Program (DMSP) satellite.

## 2.3. Ice production modelling

We construct a time series of modelled ice production per unit area as per Renfrew et al. (2002). For this, the total surface heat flux is weighted by the satellite-observed open water fraction to give  $Q_{tot}(t)$ ; oceanic cooling and thus ice production are then obtained from  $Q_{tot} = \rho_i L_f F$ , where  $\rho_i$  is the density of ice,  $L_f$  is the latent heat of fusion and  $F$  is the ice production rate. An assumption is made that ice is only produced when (1)  $Q_{tot} > 0$ , that is, heat flux is from the ocean into the atmosphere, and (2) we are within the freezing season. Outside of this period it is assumed that surface heat loss will lead to a cooling of the ocean rather than ice production. We make the assumption that the freezing season is between 15 June and 1 November; these dates were chosen according to local SSTs (Fig. 3). The onset of freezing being in mid-June also agrees well with direct observations of sea ice coverage from a remote camera on Signy Island (Fig. 4).

Daily SST values in the ice production model were prescribed from the ECMWF analyses, as per Fig. 3. These compare well with SST observations from the seal CTD during the period of overlap, especially when one considers that the ECMWF estimates are a "skin" SST (i.e. a measure of the very thin surface layer of the ocean, such as might be seen by satellite-borne radiometers), while the seal observations are of "bulk" SST (i.e. temperature typical of that measured close to the surface by *in situ* instrumentation. Note that we here define the seal-derived SST as being that at 0 dbar pressure in optimally interpolated temperature fields obtained from the seal CTD data; see below). As well as being directly weighted for ice concentration, the heat fluxes are



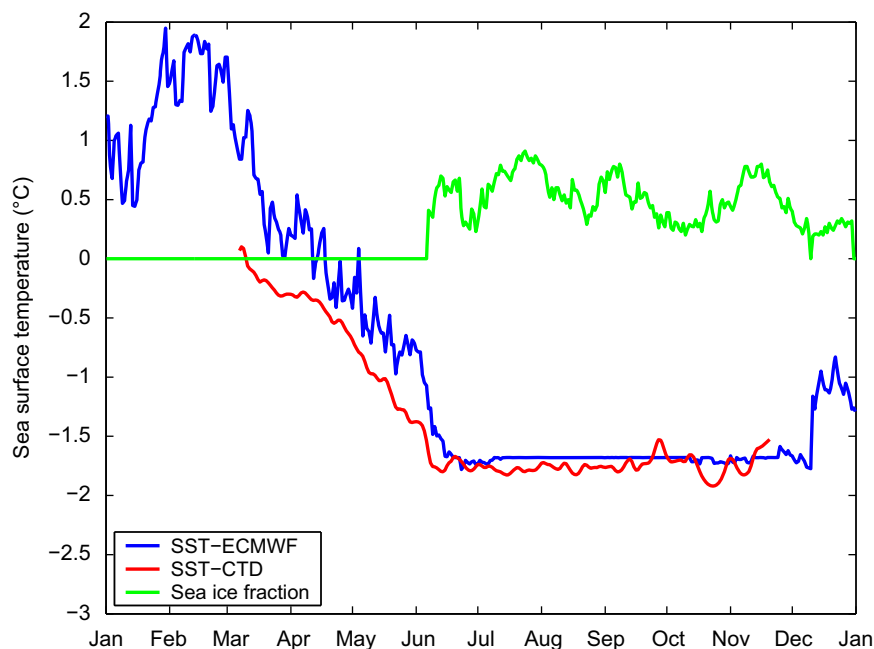


**Fig. 3.** Sea surface temperature (SST) near the South Orkney Islands in 2007 according to the ECMWF operational analyses (blue) and the CTD-SRDL *in situ* measurements (red). Based on these, the freezing season is presumed to start in mid-June, when SST reaches the surface freezing point. Also plotted is the satellite-derived sea ice fraction (green) extracted immediately to the north of the Islands.



**Fig. 4.** Selected stills taken during 2007 by the remote sea ice camera on Signy Island, South Orkneys. These were taken on May 8th (top left), June 4th (top right), June 9th (bottom left) and June 15th (bottom right). The onset of sea ice cover in mid-June is apparent.

also weighted according to ice thickness as per Renfrew et al. (2002), where ice is taken to be ‘thin’ (less than 0.3 m) when the ice fraction is less than about 0.8, and ‘thick’ (more than 0.3 m) when the ice fraction is greater than 0.8. It should be noted that the sea ice production modelling is inherently one-dimensional; it takes no account of possible advective influences.

#### 2.4. Ocean mixed-layer modelling

To simulate the upper-ocean properties that would be observed in response to solely local surface fluxes and ice production, an oceanographic mixed-layer model based on the Price–Weller–Pinkel (PWP) model (Price et al., 1986) was constructed and run. This was

forced with the air–sea fluxes derived from the meteorological dataset described above. Within the PWP model, three criteria for vertical stability are applied during each timestep; these depend on static stability, the bulk Richardson number criterion, and the gradient Richardson number criterion. Vertical advection and vertical turbulent mixing are applied subsequently. Vertical diffusivity ( $K_z$ ) is assigned a value of  $10^{-4} \text{ m}^2 \text{ s}^{-1}$ , though the results shown here are not particularly sensitive to this value. The model allows for vertical advection, but not horizontal advection or mesoscale variability. Wind stress is applied as a vector in the model to allow shear at the base of the mixed layer to influence the mixing. Incoming shortwave radiative heat flux is allowed to penetrate into the ocean a distance that depends on a double exponential function determined according to the Jerlov classification of the waters, as given in Paulson and Simpson (1977); it thus differs from the other components of heat flux, which warm or cool solely the surface of the model ocean.

To account for the impact of ice production on the simulated upper ocean, the PWP model was forced with the output of the sea ice production model described above, with sea ice formation acting to inject brine into the surface model ocean, and sea ice melt injecting freshwater. Latent heats associated with ice formation and melting were included in the heat budget applied, and it was assumed that possible glacial melt from the islands had negligible impact. Note that the same approach, of coupling a one-dimensional sea-ice production model and an ocean mixed-layer model, was adopted previously by Meredith et al. (2004) for the Marguerite Bay area of the western Antarctic Peninsula.

### 3. Results

From the spatial distribution of profiles obtained from the elephant seal during 2007 (Fig. 5), it is clear that the seal had a preferred location close to the shelf break to the northeast of the South Orkney Islands. There is very little deviation from this position during the > 8 months of data coverage. The only notable excursion occurred in October (crosses in Fig. 5), when the seal ventured beyond the shelf break and (briefly) into the open Scotia Sea. Examination of CTD data recovered from this short period shows

some significant differences, not only in the greatest depth of the profiles, but also in their potential temperature–salinity properties (not shown). These differences are consistent with the seal having moved northward into the ACC regime (specifically having crossed the SACCF; Fig. 1), and consequently these profiles have been excluded from analysis to preserve the Eulerian integrity of the time series.

For the time series obtained from the remaining profiles, we investigated the possibility of any apparent temporal signals that could actually be due to the small level of spatial variability left. This was done by constructing time series using a very rigorous spatial constraint, specifically including data from just the cluster of profiles close to the shelf break at the northeastern side of the South Orkneys (Fig. 5). There was insignificant difference between this series and that constructed using the fuller data set, so we are confident of the Eulerian nature of the data. Locations from which data were collected for this are marked by dots in Fig. 5.

The CTD–SRDL data were optimally interpolated onto a regular grid of 1-day (horizontal) by 10 dbar (vertical) to produce upper-ocean time series of potential temperature, salinity and density (Fig. 6). The time series demonstrate some clear features of the seasonal evolution of the upper water column in this locale. Near-surface waters in March had temperatures close to  $0^\circ\text{C}$ , and were underlain by a colder layer at around 200 dbar, with temperatures down to  $-0.75^\circ\text{C}$ . Deeper still lay the upper part of the Warm Deep Water (WDW), which is derived from the Circumpolar Deep Water (CDW) of the ACC but which is significantly modified during its circulation within the subpolar gyre and via injection of shelf waters into the WSC. WDW is a comparatively warm, saline water mass, which can provide heat and salt to the upper ocean by vertical mixing with overlying water masses and by being entrained into the mixed layer as it deepens seasonally.

The cold subsurface layer at around 200 dbar is termed Winter Water (WW), and is the remnant of the previous winter's mixed layer that becomes distinct from the surface waters when the latter are warmed by insolation and freshened by ice melt. By around mid-April, the surface temperatures have dropped significantly, and the WW layer is eroded; at this time, the upper ocean has a two-layer structure, with colder surface waters

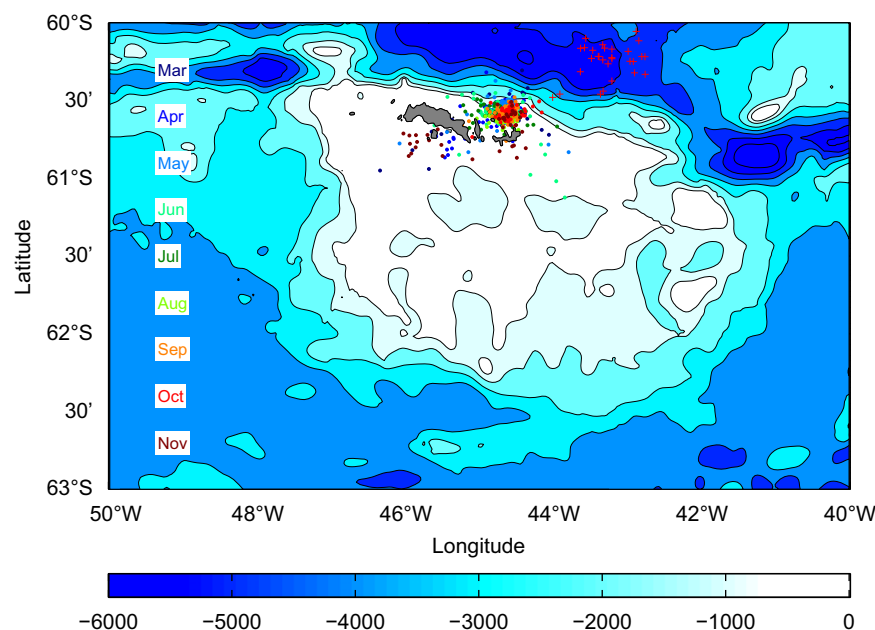


**Fig. 5.** Spatial distribution of profiles collected by the CTD–SRDL-tagged elephant seal during 2007. Profile locations are colour-coded by month. Note the brief excursion during October when the seal ventured beyond the shelf break (locations marked by crosses); these profiles are excluded from the Eulerian time series constructed.

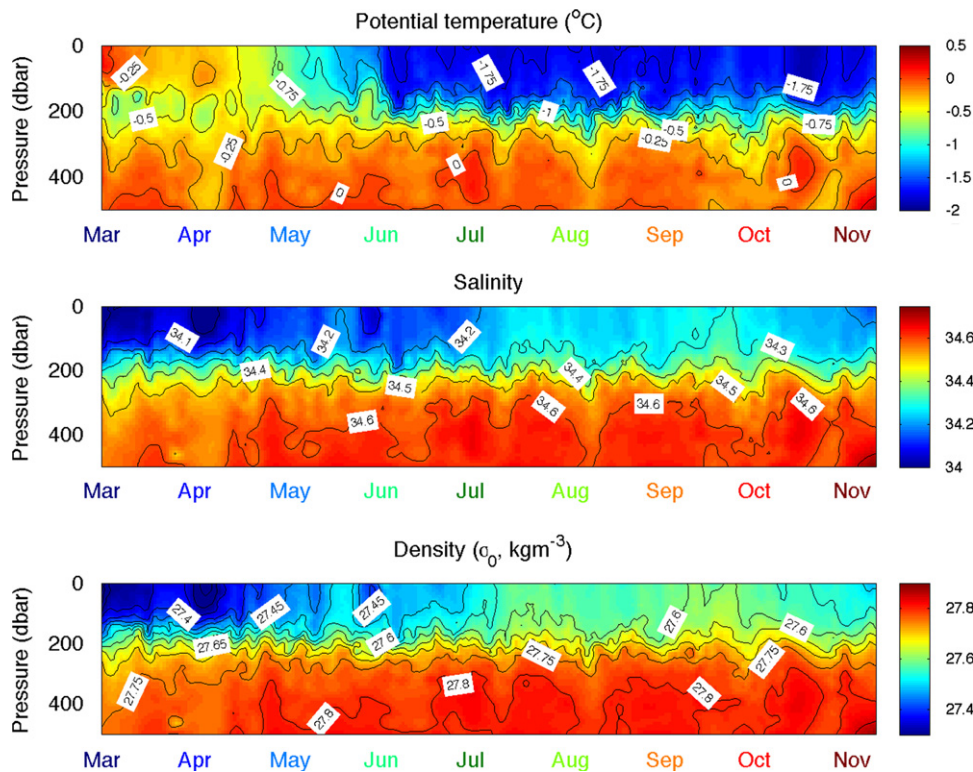


Fig. 6. Time series of potential temperature (top), salinity (middle) and potential density ( $\sigma_0$ ) for the upper ocean near the South Orkney Islands during 2007.

overlying the warmer WDW below. By June, surface temperatures approach freezing point, and there is only slight deviation from this through to November. During this period, the upper ocean constitutes a slab of cold water approximately 200 m thick.

Salinity also shows a strong seasonal progression (Fig. 6). At the start of the sequence, the surface ocean is markedly fresh (salinity around 34.0), reflecting freshwater input from melting ice during the previous summer. This overlies the more saline WDW, which has salinities higher than 34.6. The surface ocean remains relatively fresh until around May, when it starts to become more saline. With the exception of a transient freshening in June, this continues through to July/August, by which time surface salinities reach 34.2–34.3. September and October have surface salinities around this level, but there are signs of freshening toward the end of the sequence, and surface salinities drop to below 34.2 in November. The sequence of density measurements (Fig. 6) strongly resembles that of salinity, as is expected from the equation of state for seawater at low temperatures.

When viewed in potential temperature–salinity space (Fig. 7), the early part of the sequence of hydrographic data (March and April) shows the characteristic inflection that reflects the presence of WW in the summertime Southern Ocean. Data from May show a much broader envelope, reflecting changes due to the rapid surface cooling as the waters approach freezing point. By mid-June, the potential temperature–salinity curves have become essentially straight lines, with the winter mixed layer at the freezing point and a continuum of data points between this and the warmer, more saline WDW.

The temporal progression of the salinity data can be used to infer sea ice production rates, as per Charrassin et al. (2008). This calculation assumes that all measured salinification of the water column is due to brine rejection from ice formation (i.e. no local precipitation/evaporation or glacial melt input), and accounts for the different densities and salinities of seawater and sea ice. It also implicitly assumes that advective effects are negligible, i.e. that the brine rejected as the ice is produced remains *in situ* at the sampling

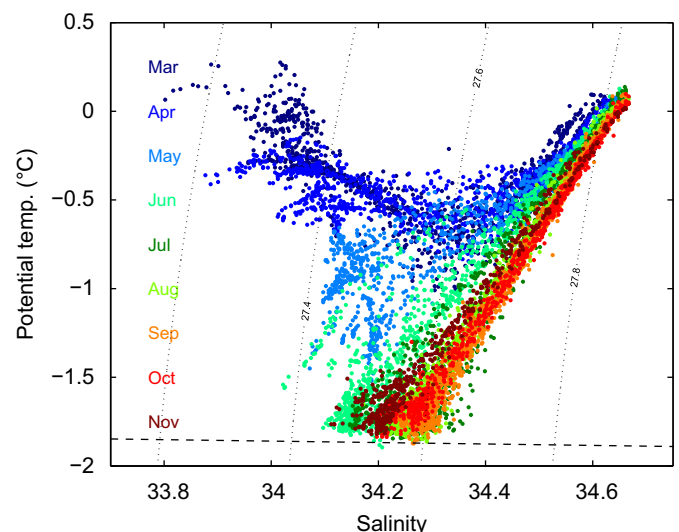


Fig. 7. Potential temperature–salinity diagram for the upper layers of the ocean near the South Orkney Islands in 2007. Data points are colour-coded by month, and locations of data collection are shown in Fig. 5. The near-horizontal dashed line denotes the freezing point of seawater.

site, and that the characteristics of the waters at the sampling site are determined locally with negligible influence from waters upstream in the regional circulation. This assumption is complicated by the likelihood of spatial gradients in salinity in the upstream regions, and the possibility of seasonal and other temporal variability in these spatial gradients. We investigate the impact of this assumption below.

The inferred rate of sea ice production (Fig. 8) was derived according to the measured changes in water column salinity, using



methodology as per Charrassin et al. (2008). For this, the upper 200 m of the data were used, since this covers the full depth over which seasonal salinity changes are seen at this site (Fig. 6). Rates of sea ice production derived this way were highest during April to July, peaking at over  $0.4 \text{ m month}^{-1}$  in July, with significant rates also observed in September. This pattern naturally reflects the observed salinification of the water column during each of these months, with the rate of salinity increase being greatest in July (Fig. 6). Note also that the data viewed in potential temperature–salinity space shows the greatest spread of salinities at the freezing point in this month (Fig. 7). However, they also show that the surface ocean was not at the freezing point during April or May, hence the inferred ice production (shown in Fig. 8) cannot be realistic for these months. We tested whether evaporation could feasibly explain some of the salinity increases in these months by converting the latent heat flux into evaporation and deriving the equivalent salinification of the upper water column that could be so produced. Values for this are very small (less than 0.003 and 0.006 in April and May, respectively), thus we conclude that evaporation did not cause the observed salinity

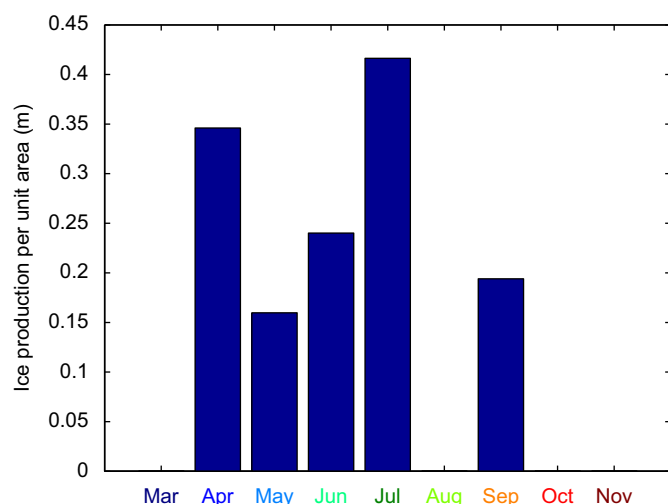


Fig. 8. Monthly sea ice production per unit area, derived from the observed salinification of the upper 200 m of the water column at the sampling site (Fig. 6).

increases. Instead, we surmise that these observed salinity changes were due instead to advective processes, with more saline water being brought to the time series location from upstream in the regional circulation. It should be noted that April and May also showed strong changes in potential temperature structure (Fig. 6), with marked cooling of the surface layers, deepening of the mixed layer, and erosion of the WW. These changes are characteristic of the impact that seasonal ice production has on the upper Southern Ocean (e.g. Meredith et al., 2004), and we theorise here that this was indeed the case, but with the caveat that the sea ice production occurred upstream with the waters affected then advected to the sampling site. In essence, we are hypothesising that the derived ice production reflects a “smeared average” of ice production from a region upstream of the South Orkneys, rather than being purely local.

To ascertain whether this is feasible, we examined the trajectories of surface drifters that were released in this region. Although this area is one marked by a paucity of data in general, and one where the sea ice field is often not conducive to Lagrangian studies of surface circulation, we were fortunate that a number of drifters were deployed upstream of the South Orkney Islands in the Weddell Sea in 2007 as part of a separate project (Fig. 9, reproduced from Thompson et al., 2009). These drifter trajectories reveal that surface waters close to the ice edge in the northwest Weddell Sea in February can reach the general vicinity of the South Orkneys on a timescale of 2–3 months. During the period February to April, the ice edge continually advanced to the north and east (Fig. 10), with the advective timescale between the ice edge and the South Orkneys progressively diminishing in response. Although none of the drifters released in 2007 actually reached our specific sampling site, the broad timing is approximately correct for waters to be advected from upstream in the Weddell Sea to bring salinified water to the site of our seal-derived series, and hence explain the anomalously early inferred sea ice production. For example, drifters that were close to the ice edge in the northwestern Weddell Sea during mid-March arrive close to the edge of the South Orkney Islands shelf by the end of April, thus if sea ice were being produced near the ice edge during March it could explain some of the salinified water observed near the South Orkneys during late April or May.

Given that advection appears to dominate the inferred sea ice production estimates during April and May, we assert that our

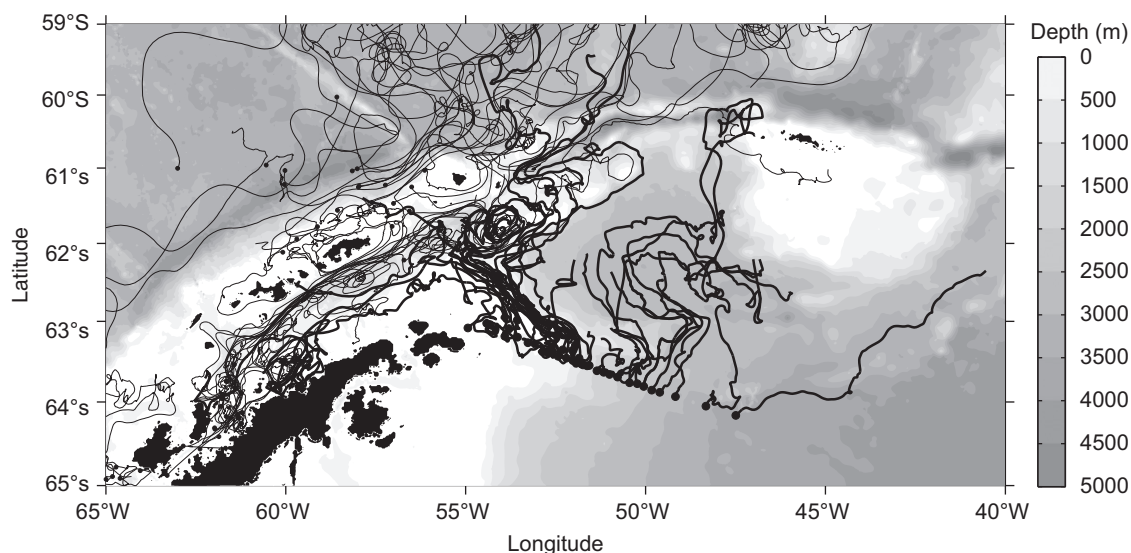
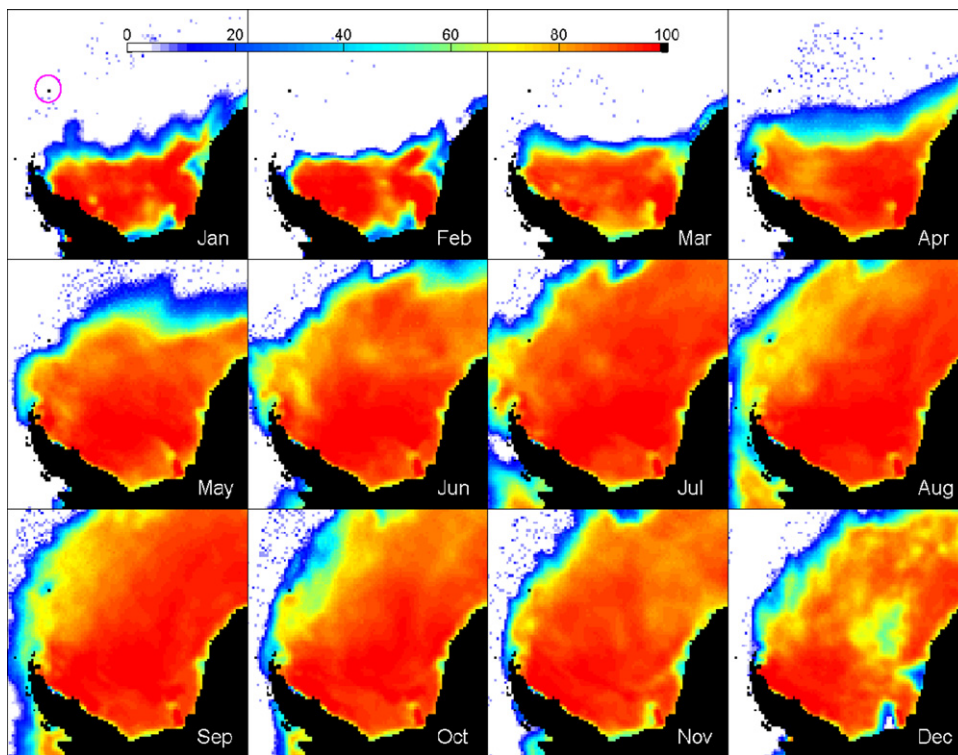


Fig. 9. Trajectories of drogued drifters deployed in the vicinity of the Antarctic Peninsula. Heavy lines denote drifters purposefully deployed in the northwest Weddell Sea by Thompson et al. (2009), light lines denote drifter trajectories from the historical database. Although none of the drifters reach the exact locality of our seal-derived oceanographic sequence, a general advective timescale of 2–3 months for them to reach the approximate vicinity of the South Orkneys was derived. Figure reproduced from Thompson et al. (2009).



**Fig. 10.** Monthly maps of sea ice concentration in the Weddell Sea sector during 2007, from the Special Scanning Microwave Imager (SSM/I). For reference, the location of the South Orkney Islands is circled in the map for January. Note the “halo” of low sea ice concentration surrounding the South Orkneys during August and September.

theory (of these estimates being “smeared averages” relevant to the upstream circulation in the Weddell Sea) is likely correct, at least for these months. This raises the question of how indicative of local ice production the inferred ice production rates from other months will be. To test this, we examined the output of the ice production model described above (Section 2.3); since this model was forced with fluxes local to the region of the South Orkneys, and hence the pattern of ice production derived this way is more likely to reflect local ice production.

Sea ice production from this model was derived (Fig. 11), and whilst there are some similarities with the pattern of ice production inferred from the seal-derived salinity data (e.g. July being the month of peak ice production), the differences are more striking. In particular, rates of ice production are in general much higher (around double), and the seasonality also differs markedly. To the extent that we believe that the ice production model results better reflect local sea ice production (as opposed to a broader upstream average), we can illustrate how the upper ocean would evolve if it were influenced solely by these local forcings (i.e. local ice production and meteorological fluxes). For this, the oceanographic mixed layer model described in Section 2.4 was run, and output analysed (Fig. 12). It is immediately clear that the temporal fields are much smoother than those seen in the observed data (Fig. 12, cf. Fig. 6); this is a reflection of the absence of mesoscale variability and other small-scale processes in the model. More interesting for us, though, are the differences in the seasonality of the data. In particular, the deepening of the winter mixed layer occurs much more rapidly in the observations than in the model output. In the latter, the layer of water with temperatures close to the freezing point deepens gradually between June and September; this contrasts with the observations (Fig. 6) where this same layer is already around 200 m thick by June. This difference is clearly due to the different seasonality in the ice production rates, and a reflection of the modelled fields being determined by local processes only, unlike the observed fields. It is also notable that the modelled upper layer

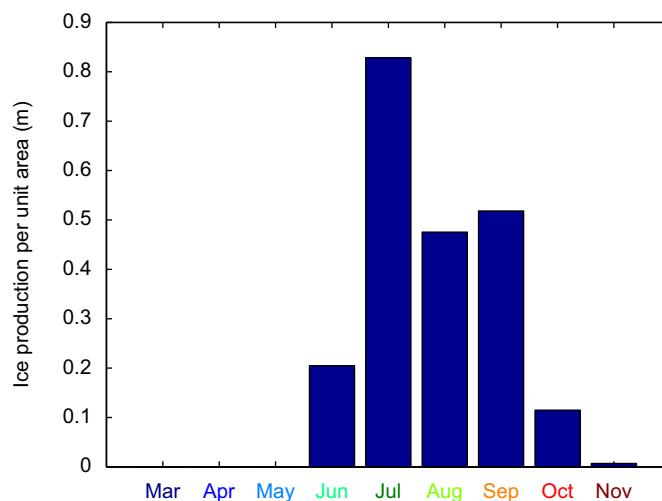


**Fig. 11.** Rates of ice production derived from the model described in Section 2.3.

salinity (and hence density) increases monotonically between June and October. This is a reflection of the ice production being uniformly positive during these months (Fig. 11), which also explains the steadiness of the deepening of the winter mixed layer.

#### 4. Discussion and conclusions

As noted by Charrassin et al. (2008), the rate of sea ice production is an important parameter to measure and understand in the Southern Ocean, but one for which there have been surprisingly few estimates produced. Those that do exist are generally confined to regions of coastal polynyas (e.g. Renfrew



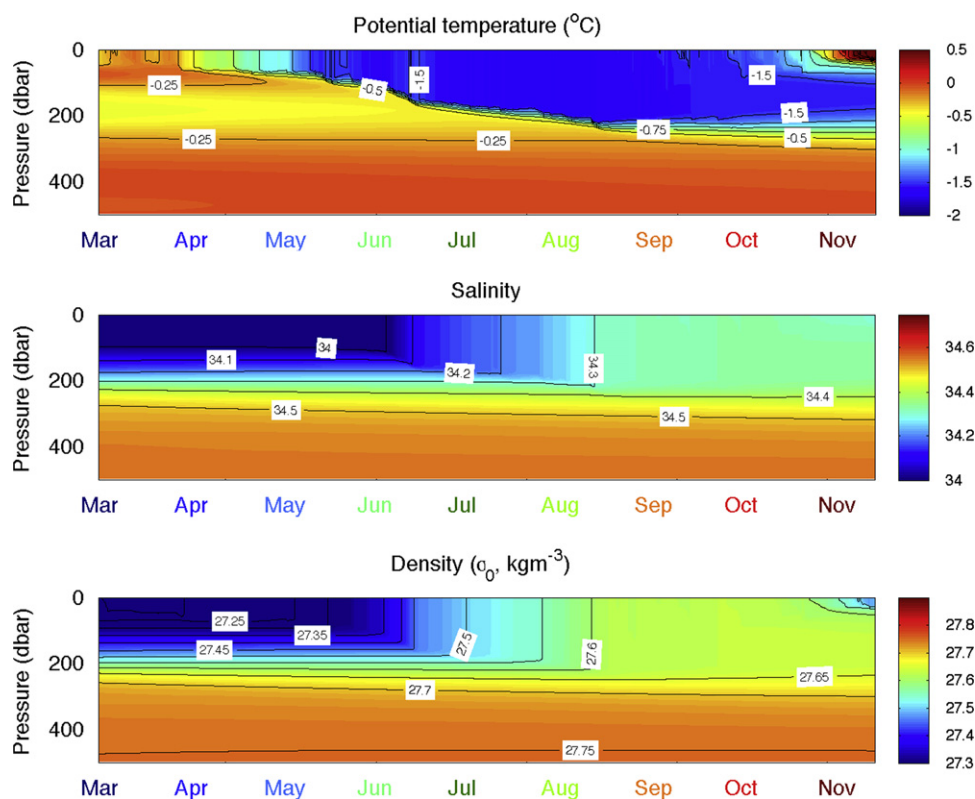


**Fig. 12.** Simulated temporal progressions of upper ocean potential temperature (top), salinity (middle) and potential density (bottom), derived from the PWP model (Section 2.4) forced with meteorological data and the output from the sea ice production model. The differences with observations (Fig. 6) are pronounced — note in particular the much slower deepening of the cold winter mixed layer, due to the later onset of modelled ice production.

et al., 2002) or landfast ice (e.g. Heil et al., 1996), and these may be unrepresentative of the broader Southern Ocean, most likely being larger and smaller than the norm, respectively. Charrassin et al. (2008) added estimates for ice production in the consolidated pack to these. For this, they used repeat hydrographic measurements from East Antarctica (between 35°E and 105°E) from the freezing season to infer production based on salinification of the upper ocean. They derived formation rates in the range  $\sim 0.7\text{--}0.9\text{ m month}^{-1}$  for April to early May,  $\sim 0.2\text{--}0.3\text{ m month}^{-1}$  for late May and  $\sim 0.3\text{ m month}^{-1}$  for May to August.

To attempt to add further quantitative information on this subject for a different region, we adopted a similar procedure to that used by Charrassin et al. (2008), applying it to a very long, serendipitously derived time series of hydrographic data recovered from close to the South Orkney Islands. We derived ice production rates of  $\sim 0.15\text{--}0.4\text{ m month}^{-1}$  for April to July, and significant values still in September (around  $0.2\text{ m month}^{-1}$ ). Our sampling location is farther from the Antarctic continent than those used by Charrassin et al. (2008) and has a correspondingly shorter period of the year covered by sea ice, however the rates of ice production that we derive are still significant.

However, interpreting these results requires care. When deriving ice production rates using the above methodology, a number of assumptions are implicit. These include an assumption of negligible precipitation/evaporation, glacial melt and advection. The first two of these seem to be generally supportable, but in our case the latter does not. Instead, we have observed significant potential for advective flow from upstream in the northwestern Weddell Sea to influence the waters at our sampling site. Against this background, we suggest that the ice production estimates we have derived better reflect averages that pertain to waters between the approximate vicinity of the tip of the Antarctic Peninsula and the South Orkney Islands, rather than being specifically local estimates.

In many respects, this broader-area average may be a more useful climatic value to measure, although its interpretation is more problematic than purely local point estimates.

We have illustrated the likely impact that advection has on these ice production estimates by contrasting them with estimates based on purely local (one-dimensional) sea ice production modelling, and by contrasting the observed temporal fields of hydrographic parameters (most pertinently salinity) with those obtained by simulating the ocean's response to purely local ice production and meteorological forcings. The differences are profound, including a factor of nearly two in the ice production rates and a much more progressive deepening of the slab of cold water that occupies the surface layers of the ocean at the sampling site during winter.

With regard to the cause of the significantly higher ice production rates obtained from modelling based on local forcings, it is worth noting that the vicinity of the South Orkneys was surrounded by a "halo" of low sea ice concentration during August and September (Fig. 10), and that this (combined with the advance and retreat of the ice pack) kept sea ice concentrations relatively low here throughout 2007 compared with other longitudes in the northern Weddell Sea. Indeed, ice concentrations here never reached 90% during 2007, and only exceeded 70% in July. Low sea ice concentrations are conducive to higher rates of sea ice production, and the contrast between the low concentrations around the South Orkneys and the much higher concentrations upstream in the Weddell Sea during the austral autumn and winter (Fig. 10) is the most likely explanation for the difference in magnitude between locally modelled ice production estimates and those inferred from the observed oceanographic data. The origin of the halo of low ice concentration around the South Orkneys is not known, but could be due to divergence of the ice field associated with the influence of the winds in the presence of the local orography, and/or topographically induced upwelling of warmer waters from below.

We do not attempt here to address the issue of longer-term (interannual) changes in sea ice production in our region of interest, since we only have observational oceanographic data from 2007. We note, however, that 2007 was an El Niño year, and it is well established that such years can show anomalous distributions in surface fluxes, SST and sea ice (e.g. Kwok and Comiso, 2002; Turner, 2004), especially at the Antarctic Peninsula and into the South Atlantic (e.g. Meredith et al., 2004, 2008). As a quick check, we examined the long sequence of air temperature records from the South Orkneys to place the 2007 measurements in the context of longer-term variability, and whilst there were no clear indications of El Niño-related anomalies in 2007, the possibility that this year may be atypical certainly remains.

In summary, we have presented new detail into the seasonal evolution of the upper water column in the vicinity of the South Orkney Islands by using an unprecedented >8-month sequence of hydrographic profiles obtained with high temporal resolution. This was possible through a combination of novel technology and the particular behaviour of the seal that was tagged. We have related these measurements to sea ice production, and inferred ice production estimates that we believe relate more to the broader-area of the northwestern Weddell Sea than to the specific locality of the South Orkney Islands. With the caveat that oceanic advection makes these ice production estimates somewhat difficult to interpret, we believe that further monitoring of the upper water column structure in this region would be beneficial, to attempt to determine interannual changes and long-term trends in ice production, and to better understand its impact on regional oceanography and circulation. If this were to be implemented, the monitoring of other parameters in addition to conventional hydrography (e.g. fluorescence, photosynthetically active radiation and/or oxygen concentrations) would be highly desirable so as to gain insight into the biogeochemical functioning of this part of the Southern Ocean as well as the physical functioning. We note that efforts are underway to develop such technologies suitable for inclusion on platforms such as the CTD-SRDL instruments. Repeating the measurements obtained here over several years will not be easy, given the unique nature of the data obtained from 2007 and the fortuitous nature of its recovery, however we believe that the comparatively low cost of data collection and significant scientific insights that might be obtained from such an extended time series make this worthy of pursuit.

## Acknowledgments

Andy Clarke (BAS) is thanked for access to the sea ice camera imagery, and much useful advice. Dave Sproson (UEA) is thanked for extracting the ECMWF operational analysis data, which has been downloaded from the British Atmospheric Data Centre. The Orcadas meteorological observations were downloaded from the British Antarctic Survey's meteorological database. Andrew Fleming from the BAS Mapping and Geographical Information Centre is thanked for assistance with the satellite sea ice data. We thank the two anonymous reviewers, whose comments helped us improve our original manuscript. Our elephant seal is thanked for being the least adventurous in the Southern Ocean. This research was funded by the Natural Environment Research Council.

## References

- Biuw, M., Boehme, L., Guinet, C., Hindell, M., Costa, D., Charrassin, J.-B., Roquet, F., Bailleul, F., Meredith, M., Thorpe, S., Tremblay, Y., McDonald, B., Park, Y.-H., Rintoul, S., Bindoff, N., Goebel, M., Crocker, D., Lovell, P., Nicholson, J., Monks, F., Fedak, M.A., 2007. Variations in behaviour and condition of a Southern Ocean top predator in relation to in situ oceanographic conditions. *Proceedings of the National Academy of Sciences* 104 (34), 13705–13710.
- Boehme, L., Thorpe, S.E., Biuw, M., Fedak, M., Meredith, M.P., 2008a. Monitoring Drake Passage with elephant seals: frontal structures and snapshots of transport. *Limnology and Oceanography* 53, 2350–2360.
- Boehme, L., Thorpe, S.E., Meredith, M.P., Biuw, M., Fedak, M., 2008b. Antarctic Circumpolar Current frontal system in the South Atlantic: monitoring using merged Argo and animal-borne sensor data. *Journal of Geophysical Research* 113 (C09012). doi:10.1029/2007JC004647.
- Charrassin, J.-B., Hindell, M., Rintoul, S.R., Roquet, F., Sokolov, S., Biuw, M., Costa, D., Boehme, L., Lovell, P., Coleman, R., Timmermann, R., Meijers, A., Meredith, M., Park, Y.-H., Bailleul, F., Goebel, M., Tremblay, Y., Bost, C.-A., McMahon, C.R., Field, I.C., Fedak, M.A., Guinet, C., 2008. Southern Ocean frontal structure and sea-ice formation rates revealed by elephant seals. *Proceedings of the National Academy of Sciences* 10.1073/pnas.0800790105.
- Clarke, A., 1988. Seasonality in the Antarctic marine environment. *Comparative Biochemistry and Physiology. Part B: Biochemistry & Molecular Biology* 90, 461–474.
- Clarke, A., Leakey, R.J.G., 1996. The seasonal cycle of phytoplankton, macronutrients, and the microbial community in a nearshore Antarctic marine ecosystem. *Limnology and Oceanography* 41 (6), 1281–1294.
- Connolley, W.M., 2002. Long-term variation of the Antarctic Circumpolar Wave. *Journal of Geophysical Research* 108 (C4). doi:10.1029/2000JC000380.
- Costa, D.P., Klinck, J.M., Hofmann, E.E., Dinniman, M.S., Burns, J.M., 2008. Upper ocean variability in west Antarctic Peninsula continental shelf waters as measured using instrumented seals. *Deep-Sea Research II* 55, 323–337.
- DeCosmo, J., Katsaros, K.B., Smith, S.D., Anderson, R.J., Oost, W.A., Bumke, K., Chadwick, H., 1996. Air–sea exchange of water vapour and sensible heat: the humidity exchange over the sea (HEXOS) results. *Journal of Geophysical Research* 101, 12001–12016.
- Falkowski, P.G., Barber, R.T., Smetacek, V., 1998. Biogeochemical controls and feedbacks on ocean primary production. *Science* 281, 200–206.
- Fedak, M.A., 2004. Marine mammals as platforms for oceanographic sampling: a “win/win” situation for biology and operational oceanography. *Memoirs of National Institute Polar Research* 58, 133–147.
- Heil, P., Allison, I., Lytle, V.I., 1996. Seasonal and interannual variations of the oceanic heat flux under a landfast Antarctic sea ice cover. *Journal of Geophysical Research* 101, 25741–25752.
- Heywood, K.J., Garabato, A.C.N., Stevens, D.P., Muench, R.D., 2004. On the fate of the Antarctic Slope Front and the origin of the Weddell Front. *Journal of Geophysical Research* 109 (C06021). doi:10.1029/2003JC002053.
- Klatt, O., Boebel, O., Fahrback, E., 2007. A profiling float's sense of ice. *Journal of Atmospheric and Oceanic Technology* 24 (7), 1301–1308.
- Korb, R., Whitehouse, M.J., Thorpe, S.E., Gordon, M., 2005. Primary production across the Scotia Sea in relation to the physico-chemical environment. *Journal of Marine Systems* 57 (3–4), 231–249.
- Korb, R.E., Whitehouse, M.J., Ward, P., 2004. SeaWiFS in the Southern Ocean: spatial and temporal variability in phytoplankton biomass around South Georgia. *Deep-Sea Research II* 51, 99–116.
- Kwok, R., Comiso, J.C., 2002. Spatial patterns of variability in Antarctic surface temperature: connections to the Southern Hemisphere Annular Mode and the Southern Oscillation. *Geophysical Research Letters* 29 (14). doi:10.1029/GL015415.
- Lydersen, C., Nøst, O.A., Kovacs, K.M., Fedak, M.A., 2004. Temperature data from Norwegian and Russian waters of the northern Barents Sea collected by free-living ringed seals. *Journal of Marine Systems* 46, 99–108.
- Lydersen, C., Nøst, O.A., Lovell, P., McConnell, B.J., Gammelsrød, T., Hunter, C., Fedak, M.A., Kovacs, K.M., 2002. Salinity and temperature structure of a freezing Arctic fjord—monitored by white whales (*Delphinapterus leucas*) 29 (23) *Geophysical Research Letters* 29 (23). doi:10.1029/2002GL015462.
- Meredith, M.P., Murphy, E.J., Hawker, E.J., King, J.C., Wallace, M.I., 2008. On the interannual variability of ocean temperatures around South Georgia, Southern Ocean: forcing by El Niño/Southern Oscillation and the Southern Annular Mode. *Deep-Sea Research II* 55 (18–19), 2007–2022.
- Meredith, M.P., Renfrew, I.A., Clarke, A., King, J.C., Brandon, M.A., 2004. Impact of the 1997/98 ENSO on the upper waters of Marguerite Bay, western Antarctic Peninsula. *Journal of Geophysical Research* 109 (C9). doi:10.1029/2003JC001784.
- Moffat, C., Beardsley, R., Owens, W.B., van Lipzig, N., 2008. A first description of the Antarctic Peninsula Coastal Current. *Deep-Sea Research II* 55 (3–4), 277–293.
- Muench, R.D., Hellmer, H.H., 2002. The international DOVETAIL program. *Deep-Sea Research II* 49, 4711–4714.
- Muench, R.D., Padman, L., Howard, S.L., Fahrback, E., 2002. Upper ocean diapycnal mixing in the northwestern Weddell Sea. *Deep-Sea Research II* 49, 4843–4861.
- Murphy, E.J., Clarke, A., Symon, C., Priddle, J., 1995. Temporal variation in Antarctic sea-ice: analysis of a long-term fast-ice record from the South Orkney Islands. *Deep-Sea Research* 42, 1045–1062.
- Orsi, A.H., Whitworth, T., Nowlin, W.D., 1995. On the meridional extent and fronts of the Antarctic Circumpolar Current. *Deep-Sea Research I* 42 (5), 641–673.
- Paulson, C.A., Simpson, J.J., 1977. Irradiance measurements in the upper ocean. *Journal of Physical Oceanography* 7, 952–956.
- Price, J.F., Weller, R.A., Pinkel, R., 1986. Diurnal cycling: observations and models of the upper ocean response to diurnal heating, cooling and wind mixing. *Journal of Geophysical Research* 91, 8411–8427.
- Renfrew, I.A., King, J.C., Markus, T., 2002. Coastal polynyas in the southern Weddell Sea: variability of the surface energy budget. *Journal of Geophysical Research* 107 (C6). doi:10.1029/12000JC000720.
- Roquet, F., Park, Y.-H., Guinet, C., Bailleul, F., Charrassin, J.-B., 2009. Observations of the Fawn Trough Current over the Kerguelen Plateau from instrumented elephant seals. *Journal of Marine Systems* 78 (3), 377–393. doi:10.1016/j.jmarsys.2008.11.017.

- Smith, S.D., 1988. Coefficients for sea surface wind stress, heat flux, and wind profiles as a function of wind speed and temperature. *Journal of Geophysical Research* 93, 15467–15472.
- Thompson, A.F., Heywood, K.J., Thorpe, S.E., Renner, A.H.H., Castro, A.T., 2009. Surface circulation at the tip of the Antarctic Peninsula from drifters. *Journal of Physical Oceanography* 39 (1), 3–26.
- Turner, J., 2004. The El Niño-Southern Oscillation and Antarctica. *International Journal of Climatology* 24, 1–31.
- Whitworth, T., Nowlin, W.D., Orsi, A.H., Locarnini, R.A., Smith, S.G., 1994. Weddell Sea Shelf Water in the Bransfield Strait and Weddell–Scotia Confluence. *Deep-Sea Research I* 41 (4), 629–641.